LABORATORY INVESTIGATION

MicroRNA expression profiling reveals the potential function of microRNA-31 in chordomas

Omer Faruk Bayrak · Sukru Gulluoglu · Esra Aydemir · Ugur Ture · Hasan Acar · Basar Atalay · Zeynel Demir · Serhat Sevli · Chad J. Creighton · Michael Ittmann · Fikrettin Sahin · Mustafa Ozen

Abstract Chordomas are rare bone tumors arising from remnants of the notochord. Molecular studies to determine the pathways involved in their pathogenesis and develop better treatments are limited. Alterations in microRNAs (miRNAs) play important roles in cancer. miRNAs are small RNA sequences that affect transcriptional and post-transcriptional regulation of gene expression in most eukaryotic organisms. Studies show that miRNA dysregulation is important for tumor initiation and progression. We compared the expression profile of miRNAs in chordomas to that of healthy nucleus pulposus samples to gain insight into the molecular pathogenesis of chordomas. Results of functional studies on one of the altered miRNAs, miR-31, are presented. The comparison between the miRNA profile of chordoma samples and the profile of normal nucleus pulposus samples suggests dysregulation of 53 miRNAs. Thirty miRNAs were upregulated in our tumor samples, while 23 were downregulated. Notably, hsa-miR-140-3p and hsa-miR-148a were upregulated in most chordomas relative to levels in nucleus pulposus cells. Two other miRNAs, hsa-miR-31 and hsa-miR-222, were downregulated in chordomas compared with the control group. Quantification with real-time polymerase chain reaction confirmed up or downregulation of these miRNAs among all samples. Functional analyses showed that hsa-miR-31 has an apoptotic effect on chordoma cells and downregulates the expression of c-MET and radixin. miRNA profiling showed that hsa-miR-31, hsa-miR-222, hsa-miR-140-3p and hsa-miR-148a are differentially expressed in chordomas compared with healthy nucleus pulposus. Our profiling may be the first step toward delineating the differential regulation of cancer-related genes in chordomas, helping to reveal the mechanisms of initiation and progression.

Keywords Chordoma · hsa-miR-31 · Microarray · miRNA · Nucleus pulposus · Skull base

Background

Chordomas are a rare type of bone tumor known to arise from notochord remnants and occurring most commonly

Sukru Gulluoglu and Esra Aydemir contributed equally to this sudy.

O. F. Bayrak · S. Gulluoglu · Z. Demir
Department of Medical Genetics, Yeditepe University Medical School and Yeditepe University Hospital, Istanbul, Turkey

S. Gulluoglu · E. Aydemir · S. Sevli · F. Sahin
Department of Biotechnology, Institute of Science, Yeditepe University, Istanbul, Turkey

U. Ture · B. Atalay
Department of Neurosurgery, Yeditepe University Hospital, Istanbul, Turkey

H. Acar
Department of Medical Genetics, Selcuklu Medical School, Konya, Turkey

C. J. Creighton · M. Ittmann · M. Ozen
Departments of Pathology & Immunology and Medicine, and Dan L. Duncan Cancer Center, Baylor College of Medicine, Houston, TX, USA

M. Ittmann
Michael E. DeBakey Department of Veterans Affairs Medical Center, Houston, TX, USA

M. Ozen (✉)
Department of Medical Genetics,
Cerrahpasa Medical School, Istanbul University,
Istanbul 3409, Turkey
e-mail: mozen@bcm.edu

🜀 Springer

around the fourth decade of life [1, 2]. This type of bone tumor is benign but it can metastasize to nearby tissues. A chordoma was first described by Virchow in 1857 as having round cells containing vacuoles [3].

Short RNA sequences of 20–30 nucleotides are known to regulate the expression of eukaryotic genes. There is growing evidence that they contribute to the initiation and progression of cancer. Differential regulation of gene expression by miRNAs has been noted in several types of cancer, including non-small-cell lung cancers, prostate cancer and breast cancer [4]. The role of miRNAs in chordomas has been recently studied, and two chordoma tissues have been used to show that hsa-miRNA-1 and hsa-miRNA-206 are differentially expressed in chordomas when compared to muscle tissue [5]. In this study, we aim to compare the miRNA expression profile of human skull-base chordoma tissues with that of nucleus pulposus tissues to determine which miRNAs might be involved in the molecular pathogenesis of chordomas.

Methods

Samples

Skull-base chordoma tissues and nucleus pulposus tissues were obtained from the Department of Neurosurgery, Yeditepe University Hospital, Istanbul, with approval from the responsible Ethics Committee of Yeditepe University Hospital. A chordoma cell line, U-CH1 generated by Silke Bruederlein at the University of Ulm, Germany, was kindly provided by the Chordoma Foundation (Durham, NC, USA).

Cell culture

For primary cell culture, eight nucleus pulposus tissue samples, obtained from patients with disc herniation, were used. These primary cultures were developed as described by Aydemir and associates [6]. Tissue samples were digested in a collagenase mix (type I, II, and IV) and incubated overnight at 37 °C. Cells were then cultured with Dulbecco's Modified Eagle Medium containing 10 % fetal bovine serum and 1 % antibiotics (100 µg/mL streptomycin and 10,000 units/mL penicillin). Once cells were attached to the culture flask, they were passaged to obtain passage 1, which was used in further experiments. The cell line U-CH1 was cultured according to the protocol described previously by Scheil [7]. U-CH1 cells with passage numbers 30–33 were grown on gelatin-coated tissue culture flasks. After reaching 80–85 % confluency, the cells were trypsinized and collected for RNA isolation.

Total RNA isolation

Total RNA from eight chordoma tissues and eight nucleus pulposus primary cultures was isolated with the TRIzol method according to the manufacturer's protocol (Invitrogen, Carlsbad, CA, USA).

miRNA microarrays

To determine the miRNA expression profiles of chordoma tissues and nucleus pulposus cells, we used microarrays consisting of 962 human and 69 human viral miRNAs, as described by Hughes and associates [8]. The Agilent Human miRNA Microarray Kit (Agilent Technologies, Santa Clara, CA, USA; Ver. 3.0, 8x15 K, 3 slides/kit, Cat.No. AGT-G4470C) was used for all experiments. The hybridization of miRNAs to the chips was performed according to the manufacturer's protocol. The slides were then washed and scanned with a double-channel axon laser scanner, the Genepix 4100A Microarray (Molecular Devices, Sunnyvale, CA, USA) and the intensity of the signal from every spot was calculated with GenePixPro Acquisition and Analysis microarray software (Molecular Devices, Sunnyvale, CA).

Data analysis

Array data were normalized by quantiles. Two-sided t tests and fold changes (using log-transformed data) were used to determine differentially expressed miRNAs. Analysis with Java TreeView represent expression values as color maps, in which multiple array probes referring to the same miRNA were first averaged [9].

Expression analysis for quantification of selected miRNAs

The expression levels of four miRNAs (hsa-miR-222, hsa-miR-140-3p, hsa-miR-148a and hsa-miR-31) differed according to microarray analysis between chordoma and nucleus pulposus samples. These differences were real-time polymerase chain reaction (PCR) using primers obtained from Exiqon (Vedbaek, Denmark). First, cDNA was synthesized from all miRNA samples according to the manufacturer's protocol (Exiqon,Cat. No.: 203300). All of the reagents, including the enzyme mix, miRNAs, and reaction buffer, were mixed and incubated at 42 °C for 60 min. These newly synthesized cDNAs were used as templates for gene-expression analysis through real-time PCR by simply combining the reaction buffer, primer mix, and cDNA in a 96-well plate (Roche, Cat. No.: 04729 692001).

Data analysis

The data were analyzed using the $2^{-\Delta\Delta Ct}$ method. During real-time PCR, spike-in control and primers were used to evaluate the efficacy of the procedure. For normalization, 5S RNA was used as a control. Statistical analysis was performed with Student's t test.

Transfection of hsa-miR-31

Ambion FAM3 Dye-Labeled Pre-miR Negative Control #1 (Life Technologies) was used to evaluate the ability of X-tremeGENE siRNA Transfection Reagent (Roche, Cat. No.: 04476093001) to transfect U-CH1 cells. After transfection, cells were imaged with a fluorescence microscope. After this validation, hsa-miR-31 (Ambion Pre-miR miR-NA Precursors PM: 114065) was transfected into U-CH1 cells with the X-tremeGENE siRNA Transfection Reagent (Roche,Cat.No. 04476093001) according to the manufacturer's protocol. To control the efficiency of transfection and to determine the intracellular availability of hsa-miR-31, total RNA isolation and miRNA reverse transcription was performed and followed by real-time PCR. The level of hsa-miR-31 was measured at 8, 16, 24, 48, and 72 h after transfection. The control groups were the X-treme-GENE group, in which only the transfection reagent and medium were delivered to cells, the scrambled miRNA group (Ambion Pre-miR miRNA Precursor Molecules—Negative Control #1), and the negative control group, which contained only medium.

Proliferation assay

To evaluate the effect of hsa-miR-31 on proliferation, the CellTiter 96 AQueous One Solution Cell Proliferation Assay (Promega, Fitchburg, WI) was used. MTS analysis was performed at 24, 48, 72 and 96 h after transfection of hsa-miR-31 on cells grown on six-well plates. The control groups were the X-tremeGENE group, in which only the transfection reagent and medium was delivered to cells, the scrambled miRNA group (Ambion Pre-miR miRNA Precursor Molecules—Negative Control #1), and the negative control group, which contained only medium. Proliferation of U-CH1 cells was assessed by measuring the absorbance at 490 nm with an ELx800 Elisa micro-plate reader (Bio-Tek, Winooski, VT). All means and standard deviations were calculated with the Microsoft Excel 2007 SR-2 software package.

Annexin V staining

To elucidate the apoptotic effects of hsa-miR-31 on chordoma cells, annexin V (Roche; Cat.No. 03703126001)

staining was performed 48–96 h after transfection of hsa-miR-31 into U-CH1 cells. Staining was carried out according to the manufacturer's protocol.

Flow cytometry

To evaluate apoptosis and necrosis with flow cytometry, the hsa-miR-31 precursor (Ambion Pre-miR miRNA Precursors PM: 114065) was transfected into U-CH1 cells in six-well plates using X-tremeGENE siRNA Transfection Reagent (Roche, Cat. No. 04476093001) according to the manufacturer's protocol. Incubation for 72 and 120 h was followed by staining with annexin V and propidium iodide according to the manufacturer's protocol (BD Pharmingen, Cat.No. 556547). Samples were run on the FACSCalibur flow cytometry device (Becton–Dickinson, Cat. No. 342975).

hsa-miR-31 target genes

To detect oncogene targets that potentially play important roles in chordoma initiation and progression in U-CH1 cells (PIK3C2A, MET, SEPHS1), a validated target (RDX) was selected using online miRNA databases, followed by refinement with Ingenuity Systems (Redwood City, CA). The expression level of the selected target genes was measured at 8, 16, 24, 48, and 72 h after transfection using two-step real-time PCR using TaqMan Gene Expression Assays (Applied Biosystems, Foster City, CA, USA). The control groups were the X-tremeGENE group, in which only the transfection reagent and medium were delivered to the cells, the scrambled miRNA group (Ambion Pre-miR miRNA Precursor Molecules—Negative Control #1), and the negative control group, which contained only medium. GAPDH was used to normalize samples. The data was analyzed with the $2^{-\Delta\Delta Ct}$ method.

Results

Differential expression of miRNAs in chordoma samples

To determine whether there are differences in the levels of miRNA expression between chordoma and nucleus pulposus tissues, we analyzed miRNAs from eight chordoma tissues and a chordoma cell line (U-CH1) and compared them with miRNAs from eight nucleus pulposus tissues (as the healthy control group). Our results show that 91 miR-NAs were expressed in both groups. Fifty-three of the 1,031 miRNAs were differentially expressed in chordoma with $P < 0.01$ and a fold change >1.5 compared with expression in nucleus pulposus tissues (Fig. 1a). The

chordoma tissue group and the cell line U-CH1 show uniform expression patterns. Of the 53 miRNAs that were significantly differentially expressed, 30 were upregulated and 23 were downregulated compared with miRNA expression levels in the nucleus pulposus samples. Furthermore, four cancer-related miRNAs were differentially expressed by more than four-fold between chordomas and the control group. Among them, hsa-miR-31 and hsa-miR-222 were significantly downregulated and miR-148 and miR-140-3p were significantly upregulated in chordoma samples ($P < 0.05$).

Validation of microarray results by real-time PCR

Selected miRNA microarray results (hsa-miR-31, hsa-miR-140-3p, hsa-miR-148a, and hsa-miR-222) were verified by real-time reverse transcription PCR (RT-PCR) using RNAs from chordoma and nucleus pulposus tissues (eight
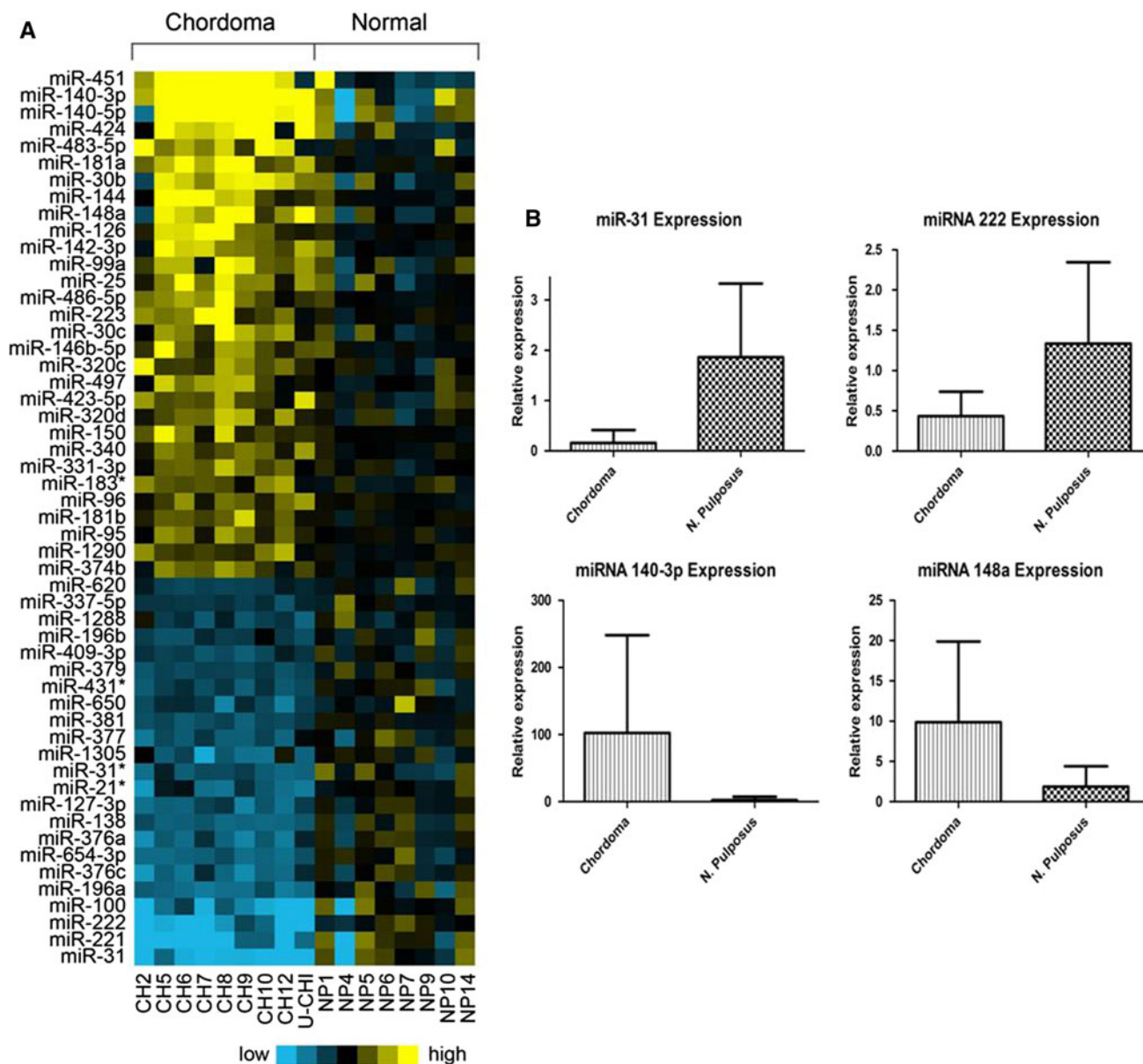

Fig. 1 Differentially expressed miRNAs. **a** A heat-map representation of expression patterns of the differentially expressed miRNAs in chordoma versus nucleus pulposus samples. Rows of the heat map represent miRNAs; columns show profiled tumors and the control (normal) group comprises nucleus pulposus samples. Relative expression is represented as a colorgram (*yellow*: high expression).

CH chordoma samples, *NP* nucleus pulposus samples, *U-CH1* a chordoma cell line. **b** The expression of four different miRNAs as determined by real time RT-PCR analysis. Shown are comparisons of the average relative expression levels of hsa-miR-31 *(a)*, hsa-miR-140-3p *(b)*, hsa-miR-148a *(c)* and hsa-miR-222 *(d)* in chordoma and nucleus pulposus samples

samples for each) and from the chordoma cell line, U-CH1. As shown in Fig. 1b, the expression levels of hsa-miR-31 and hsa-miR-222 were significantly lower in chordoma samples than in the control group whereas expression levels of hsa-miR-140-3p and hsa-miR-148a were significantly higher in chordoma samples compared to the control group.

hsa-miR-31 transfection

The transfection capability of the X-tremeGENE siRNA Transfection Reagent, when used with U-CH1 cells, was evaluated by using Ambion FAM3 Dye-Labeled Pre-miR Negative Control #1. Fluorescence microscopy showed that the FAM-labeled miRNA constructs were successfully transfected into cells (Fig. 2). Therefore, transfections were carried out with the X-tremeGENE siRNA Transfection Reagent.

After transfection, real-time PCR was performed to show the presence and processability of the transfected hsa-miR-31. RNA samples were isolated from U-CH1 cells, eight, 16, 24, 48, and 72 h after transfection by hsa-miR-31. Results showed that the hsa-miR-31 expression level was highest eight hours after transfection. The hsa-

miR-31 expression level then decreased gradually until day four (Fig. 3a).

hsa-miR-31 and the proliferation of U-CH1 cells

To investigate the effect of hsa-miR-31 on the proliferation of U-CH1 cells, MTS tests were performed. Seventy-two hours after hsa-miR-31 transfection, U-CH1 cell viability was reduced by 27 % (Fig. 3b).

hsa-miR-31 and apoptosis in U-CH1 cells

To further examine the decreased proliferation of U-CH1 cells after hsa-miR-31 transfection, hsa-miR-31-transfected U-CH1 cells were stained with annexin V to evaluate the apoptotic effects of hsa-miR-31. Light microscopy revealed that the abundance of annexin V-stained cells was significantly higher in transfected cells compared to non-transfected controls. The number of annexin V-positive cells was higher 72 h after transfection compared to that at 48 h (data not shown). Flow cytometry revealed that hsa-miR-31-transfected cells have a significantly higher apoptosis rate after 72 and 120 h compared to non-transfected cells (Fig. 3c).
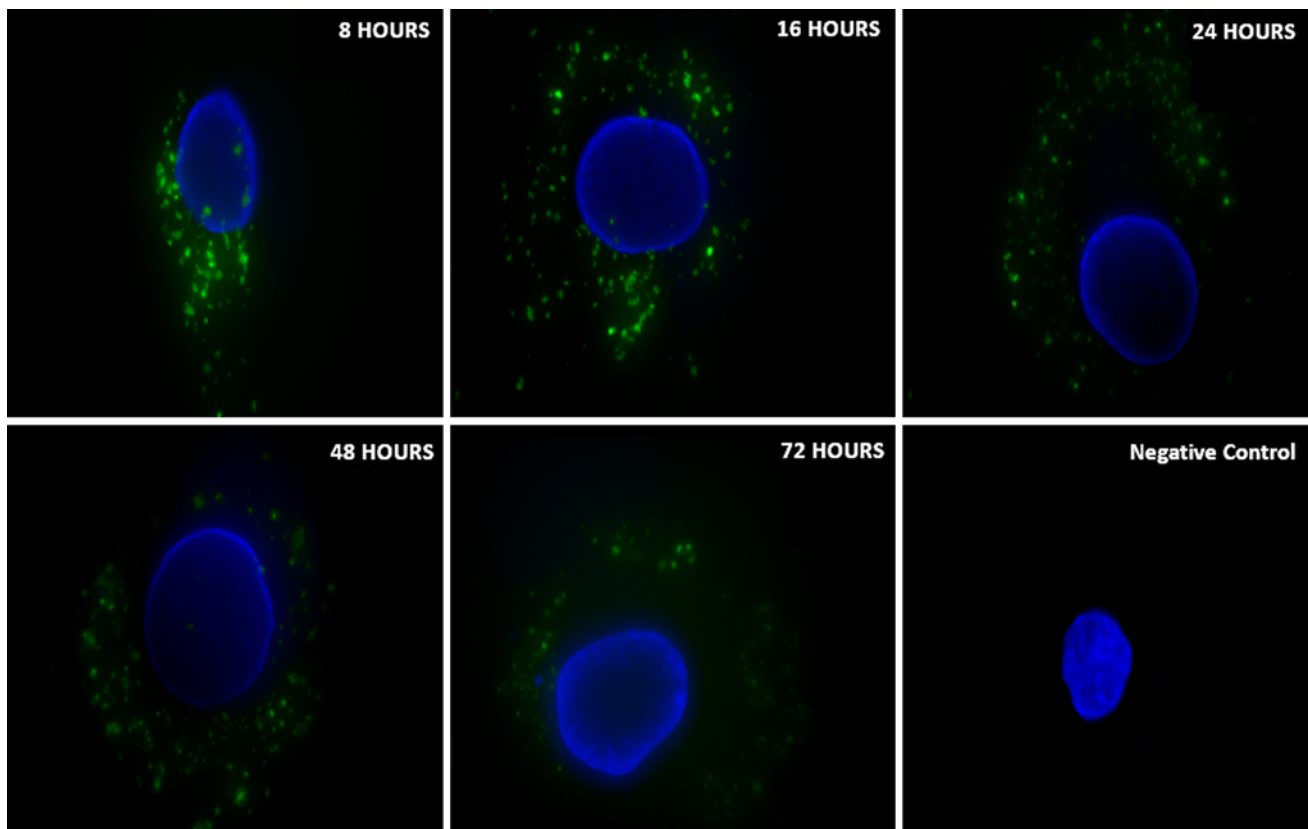

Fig. 2 FAM-conjugated scrambled miRNA molecules were transfected into U-CH1 cells for direct observation of cellular uptake. The *green spots* represent FAM-labeled miRNAs and the nucleus is stained with DAPI (*blue*)
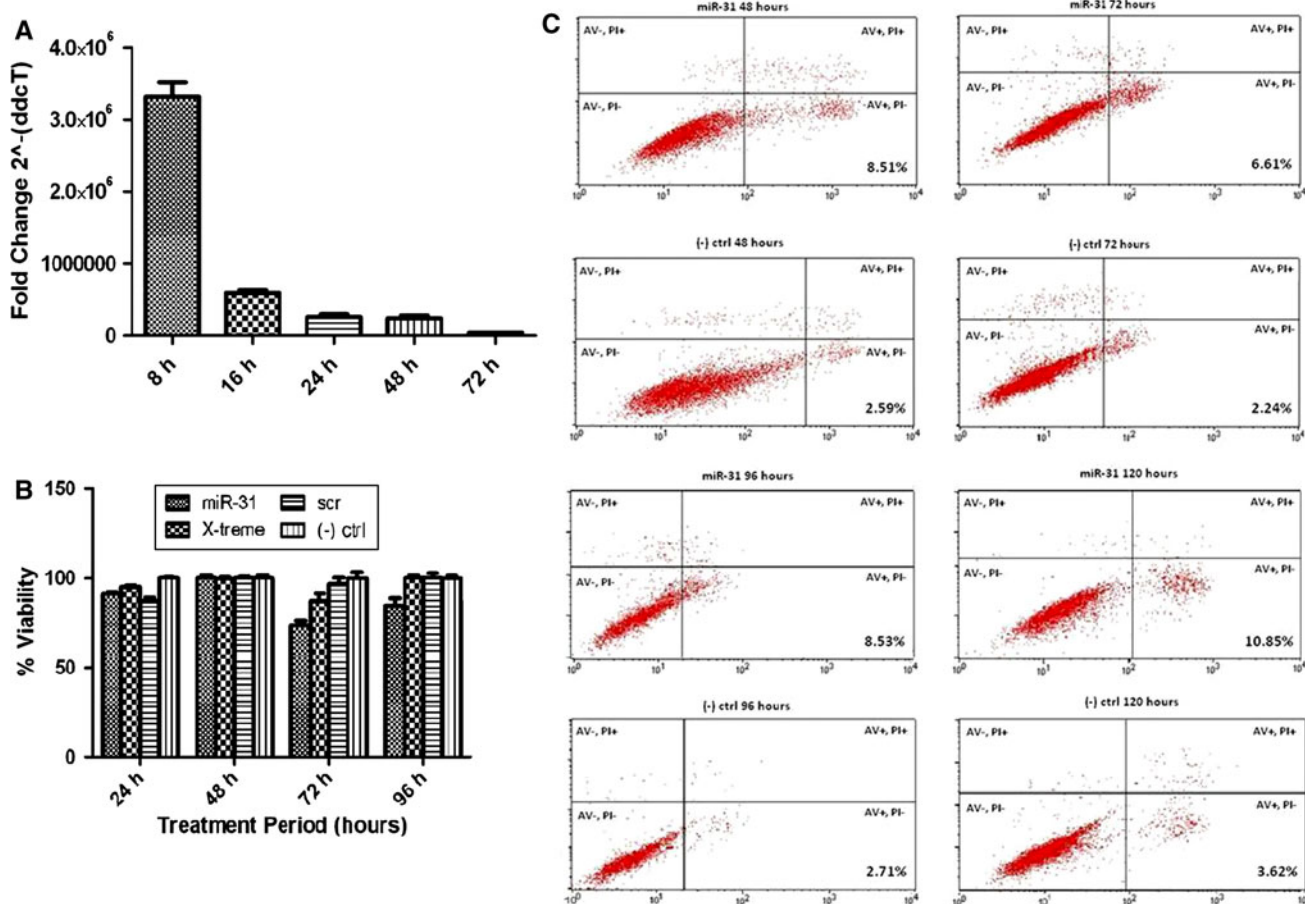
Fig. 3 **a** Expression of hsa-miR-31 at 8, 16, 24, 48 and 72 h after transfection into U-CH1 cells. **b** MTS cell proliferation results following transfection of hsa-miR-31 into U-CH1 cells. **c** *Dot plot* showing Annexin/PI staining of U-CH1 cells grown on six-well plates for 48, 72,96 and 120 h after transfection. The percentages in the lower right quadrant indicate the positively-stained cells that are in the early apoptotic stage

hsa-miR-31 and the expression of c-MET and radixin

RT-PCR analysis revealed that hsa-pre-miR-31 transfection decreases the relative expression of its predicted target, c-MET, and its confirmed target, radixin, in U-CH1 cells. Relative c-MET expression was lowest after 48 h (44 %) and relative radixin expression was as low as 75 % after 16 and 24 h. The changes in PIK3C2A and SEPHS1 expression were insignificant (Fig. 4). No significant increase or decrease was observed upon scrambled miRNA transfection (data not shown).

Discussion

Chordoma, a rare type of bone tumor originating from notochord remnants, is a slow growing malignancy. Because it is rare, few molecular studies have been reported that would enable the development of novel strategies to treat chordomas. MiRNAs are known to play a role in post-transcriptional gene silencing in almost all eukaryotes. They can act as tumor suppressors as well as oncogenes in many cancer types, including prostate cancer [10], colorectal cancer [11], and chronic lymphocytic leukemia [12].

To date, only one miRNA study of chordomas has been reported. The study used two chordoma tissue samples and a cell line, U-CH1. The control group consisted of muscle cells. The study showed that hsa-miR-1 is downregulated in chordomas relative to muscle cells. A number of studies show that miR-1 and miR-206 are specific to muscle cells [13–18]. Our study, however, compared chordoma cells and chordoma tissues with nucleus pulposus samples, which we believe to be a better reference because both chordoma and nucleus pulposus originate from the remnants of notochord at the embryonic stage [19].

Valastyan and colleagues have shown that overexpression of hsa-miR-31 inhibits the metastasis of breast cancer [20]. Another study revealed that downregulation of hsa-miR-31 is a prognostic marker in medulloblastoma [21].
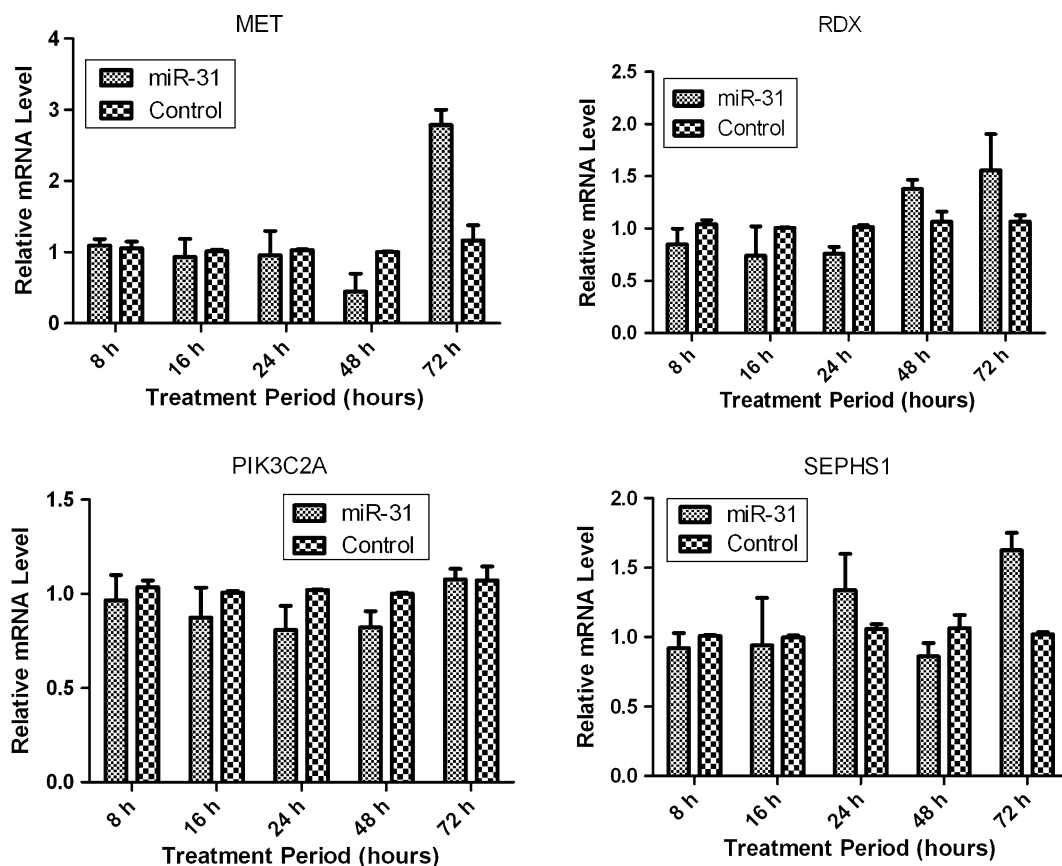
Fig. 4 Relative mRNA levels of predicted and confirmed targets of miR-31 by RT-PCR at 8, 16, 24, 48 and 72 h after transfection

Creighton and associates have shown a possible mechanism of inhibition for miR-31 through its association with p53 in serous ovarian carcinomas and other cancers [22]. In our study, eight chordoma tissues and a chordoma cell line were analyzed through miRNA microarray expression profiling to enable comparisons to be made with profiles of nucleus pulposus primary cell cultures. We found that hsa-miR-31 was significantly downregulated in chordomas. Furthermore, we found that overexpression of miR-31 decreases the number of viable chordoma cancer cells (Fig. 3b).

We observed with flow cytometry that the decrease in viability is mostly due to apoptosis, potentially caused by hsa-miR-31. The transformation of U-CH1 cells with pre-miR-31 resulted in the downregulation of c-MET and radixin. Along with other receptor tyrosine kinases, MET overexpression has been correlated with mitogenic and transforming functions through tyrosine kinase phosphorylation [23]. MET overexpression is related to invasion, evasion from apoptotic signals, angiogenesis, and cell scattering, and tumors depend on continuous MET stimulation [24]. Major efforts to produce inhibitors of c-MET and its unique ligand, HGF, are being made and phase III trials are ongoing. Among malignant bone tumors, c-MET

expression was most frequently observed in chordomas (94.4 %) [25]. Our results suggest that the low level of miR-31 in chordoma tissues, or in any other cancer, may be associated with the increased level of MET expression. Further research is required to clarify whether the downregulation of MET by miR-31 is through direct targeting or through a cascade of molecular events.

Radixin is a confirmed target of hsa-miR-31. Overexpression of the closely related ezrin, radixin, and moesin genes is associated with cell transformation, cell survival, cell motility and tumor invasion [26–28]. Our data shows that the hsa-miR-31 transfection of U-CH1 cells decreased radixin expression in the first 24 h. We also show that hsa-miR-222 is also downregulated in chordoma cells. As hsa-miR-222 is known to induce early entry into the S-phase of the cell cycle and lead to the proliferation of cancer cells, this finding may be an important step in explaining the slow growth of chordomas [29]. In many types of tumors, including papillary thyroid carcinoma, pancreatic carcinomas and glioblastomas, miR-222 has been shown to be upregulated. One study identified miR-222 and its paralog miR-221 as an epithelial-to-mesenchymal transition marker in breast cancer, noting that an increase in miR-221/222 levels decreases the expression of epithelial-specific

genes and increases the expression of mesenchymal-specific genes. This transition results in increased cell migration and invasion [30]. The observed low level of miR-222 in chordomas may also explain the low metastatic potential of the tumor.

Two other important miRNAs related to cancer were upregulated in chordomas. The first, which plays a strong role in the staging of a tumor, is miR-148a; the second, hsa-miR-140-3p, was found to be downregulated in male breast cancer [31]. More functional studies are needed to determine the targets of these miRNAs and their significance in chordoma pathogenesis. Further miRNA profiling studies with sacral and mobile spine chordomas would be useful to reveal molecular differences between these chordoma types, which are known to be biologically different.

Conclusions

To date, there has been only one other study of miRNA expression in chordomas, which compared two chordoma samples with muscle tissue. In our study, eight chordoma tumors were compared with eight nucleus pulposus samples, which we believe is a more representative healthy tissue control. Our study shows that hsa-miR-31 and hsa-miR-222 are downregulated and that hsa-miR-148 and hsa-miR-140-3p are upregulated in chordomas. These findings provide a platform to delineate the differential regulation of cancer-related genes in chordoma tumor cells. This information can help define the complex molecular biology of the initiation and progression mechanisms of the disease. In addition, MET, as a predicted target of miR-31, was found to be downregulated in U-CH1 cells after transient transfection of miR-31.Further studies are needed to uncover the molecular consequences of dysregulated miRNAs in chordomas.

References

1. Almefty K, Pravdenkova S, Colli BO, Al-Mefty O, Gokden M (2007) Chordoma and chondrosarcoma: similar, but quite different, skull base tumors. Cancer 110:2457–2467. doi:10.1002/cncr.23073

2. Clabeaux J, Hojnowski L, Valente A, Damron TA (2008) Case report: parachordoma of soft tissues of the arm. Clin Orthop Relat Res 466:1251–1256. doi:10.1007/s11999-008-0125-7

3. Wright D (1967) Nasopharyngeal and cervical chordoma–some aspects of their development and treatment. J Laryngol Otol 81:1337–1355

4. Yu SL, Chen HY, Chang GC et al (2008) MicroRNA signature predicts survival and relapse in lung cancer. Cancer Cell 13:48–57. doi:10.1016/j.ccr.2007.12.008

5. Duan ZF, Choy E, Nielsen GP, Rosenberg A, Iafrate J, Yang C, Schwab J, Mankin H, Xavier R, Hornicek FJ (2010) Differential expression of microRNA (miRNA) in chordoma reveals a role for miRNA-1 in Met expression. J Orthop Res 28:746–752. doi:10.1002/jor.21055

6. Aydemir E, Bayrak OF, Sahin F, Atalay B, Kose GT, Ozen M, Sevli S, Dalan AB, Yalvac ME, Dogruluk T, Türe U (2012) Characterization of cancer stem-like cells in chordoma. J Neurosurg 116:810–820. doi:10.3171/2011.12.JNS11430

7. Scheil S, Bruderlein S, Liehr T, Starke H, Herms J, Schulte M, Moller P (2001) Genome-wide analysis of sixteen chordomas by comparative genomic hybridization and cytogenetics of the first human chordoma cell line, U-CHI. Gene Chromosome Cancer 32:203–211

8. Hughes TR, Mao M, Jones AR et al (2001) Expression profiling using microarrays fabricated by an ink-jet oligonucleotide synthesizer. Nat Biotechnol 19:342–347

9. Saldanha AJ (2004) Java treeview–extensible visualization of microarray data. Bioinformatics 20:3246–3248. doi:10.1093/bioinformatics/bth349

10. Ozen M, Creighton CJ, Ozdemir M, Ittmann M (2008) Widespread deregulation of microRNA expression in human prostate cancer. Oncogene 27:1788–1793. doi:10.1038/sj.onc.1210809

11. Ng EK, Chong WW, Jin H, Lam EK, Shin VY, Yu J, Poon TC, Ng SS, Sung JJ (2009) Differential expression of microRNAs in plasma of patients with colorectal cancer: a potential marker for colorectal cancer screening. Gut 58:1375–1381. doi:10.1136/gut.2008.167817

12. Frenquelli M, Muzio M, Scielzo C, Fazi C, Scarfò L, Rossi C, Ferrari G, Ghia P, Caligaris-Cappio F (2010) MicroRNA and proliferation control in chronic lymphocytic leukemia: functional relationship between miR-221/222 cluster and p27. Blood 115:3949–3959. doi:10.1182/blood-2009-11-254656

13. Anderson C, Catoe H, Werner R (2006) MIR-206 regulates connexin43 expression during skeletal muscle development. Nucleic Acids Res 34:5863–5871. doi:10.1093/nar/gkl743

14. Chen JF, Mandel EM, Thomson JM, Wu Q, Callis TE, Hammond SM, Conlon FL, Wang DZ (2006) The role of microRNA-1 and microRNA-133 in skeletal muscle proliferation and differentiation. Nat Genet 38:228–233. doi:10.1038/ng1725

15. Kim HK, Lee YS, Sivaprasad U, Malhotra A, Dutta A (2006) Muscle-specific microRNA miR-206 promotes muscle differentiation. J Cell Biol 174:677–687. doi:10.1083/jcb.200603008

17. Yuasa K, Hagiwara Y, Ando M, Nakamura A, Takeda S, Hijikata T (2008) MicroRNA-206 is highly expressed in newly formed muscle fibers: implications regarding potential for muscle regeneration and maturation in muscular dystrophy. Cell Struct Funct 33:163–169

18. Xu C, Lu Y, Pan Z, Chu W, Luo X, Lin H, Xiao J, Shan H, Wang Z, Yang B (2007) The muscle-specific microRNAs miR-1 and miR-133 produce opposing effects on apoptosis by targeting HSP60, HSP70 and caspase-9 in cardiomyocytes. J Cell Sci 120(Pt 17):3045–3052. doi:10.1242/jcs.010728

19. Choi KS, Cohn MJ, Harfe BD (2008) Identification of Nucleus Pulposus Precursor Cells and Notochordal Remnants in the Mouse: implications for Disk Degeneration and Chordoma Formation. Dev Dyn 237:3953–3958. doi:10.1002/dvdy.21805

20. Valastyan S, Reinhardt F, Benaich N, Calogrias D, Szász AM, Wang ZC, Brock JE, Richardson AL, Weinberg RA (2009) A pleiotropically acting microRNA, miR-31, inhibits breast cancer metastasis. Cell 137:1032–1046. doi:10.1016/j.cell.2009.03.047

21. Ferretti E, De Smaele E, Po A et al (2009) MicroRNA profiling in human medulloblastoma. Int J Cancer 124:568–577. doi:10.1002/ijc.23948

22. Creighton CJ, Fountain MD, Yu Z et al (2010) Molecular profiling uncovers a p53-associated role for microRNA-31 in inhibiting the proliferation of serous ovarian carcinomas and other cancers. Cancer Res 70:1906–1915

23. de Luca A, Arena N, Sena LM, Medico E (1999) Met overexpression confers HGF-dependent invasive phenotype to human thyroid carcinoma cells in vitro. J Cell Physiol 180:365–371

24. Comoglio PM, Giordano S, Trusolino L (2008) Drug development of MET inhibitors: targeting oncogene addiction and expedience. Nat Rev Drug Discov 7:504–516. doi:10.1038/nrd2530

25. Naka T, Iwamoto Y, Shinohara N, Ushijima M, Chuman H, Tsuneyoshi M (1997) Expression of c-met proto-oncogene product (c-MET) in benign and malignant bone tumors. Mod Pathol 10:832–838

26. Hua D, Ding D, Han X, Zhang W, Zhao N, Foltz G, Lan Q, Huang Q, Lin B (2012) Human miR-31 targets radixin and inhibits migration and invasion of glioma cells. Oncol Rep 27:700–706. doi:10.3892/or.2011.1555

27. Valderrama F, Thevapala S, Ridley AJ (2012) Radixin regulates cell migration and cell–cell adhesion through Rac1. J Cell Sci 125(Pt 14):3310–3319. doi:10.1242/jcs.094383

28. Zheng B, Liang L, Huang S et al (2012) MicroRNA-409 suppresses tumour cell invasion and metastasis by directly targeting radixin in gastric cancers. Oncogene 31:4509–4516. doi:10.1038/onc.2011

29. Medina R, Zaidi SK, Liu CG, Stein JL, van Wijnen AJ, Croce CM, Stein GS (2008) MicroRNAs 221 and 222 bypass quiescence and compromise cell survival. Cancer Res 68:2773–2780. doi:10.1158/0008-5472.CAN-07-6754

30. Stinson S, Lackner MR, Adai AT (2011) TRPS1 targeting by miR-221/222 promotes the epithelial-to-mesenchymal transition in breast cancer. Sci Signal 4:ra41. doi:10.1126/scisignal.2001538

31. Fassan M, Baffa R, Palazzo JP et al (2009) MicroRNA expression profiling of male breast cancer. Breast Cancer Res 11:R58. doi:10.1186/bcr2348